

# Results From the Apollo Passive Seismic Experiment<sup>1</sup>

Gary Latham, Yosio Nakamura, James Dorman,  
Frederick Duennebier, Maurice Ewing,  
and David Lammlein  
*Marine Science Institute  
Division of Solid Earth  
and Planetary Geophysics  
University of Texas  
Galveston, Texas*

Recent results from the Apollo Seismic Network suggest that (1) primitive differentiation occurred in the outer shell of the Moon to a depth of approximately 300 km and (2) the central region of the Moon is presently molten to a radius of between 200 and 300 km. If early melting to a depth of 300 to 400 km was a consequence of accretional energy, very short accretion times are required. The best model for the zone of original differentiation appears to be a crust 40 to 80 km thick, ranging in composition from anorthositic gabbro to gabbro, and overlying an ultramafic cumulate (olivine-pyroxene) about 250 km thick. The best candidate for the molten core appears to be iron or iron sulphide. A new class of seismic signals has recently been identified that may correspond to shallow moonquakes. These are rare, but much more energetic than the more numerous, deep moonquakes.

Five seismic stations have been placed on the Moon by the astronauts of Apollo missions 11, 12, 14, 15, and 16. The Apollo 11 station, powered by solar cells and intended for operation only during the lunar day, failed after exposure to the first nighttime period. The remaining four stations, powered by radio isotope thermal generators (RTG), have operated continuously since their initial activation. These four stations constitute the Apollo Seismic Network. The locations and installation dates of these stations are given in table 1.

The network was completed as of April 1974, with the installation of the fourth station in the Descartes region of the southern highlands during mission 16. It is estimated that the maximum lifetime of each station will be about 10 yr, corresponding to the useful lifetime of the RTG power source. Each

station contains four seismometers. Three of these seismometers form a triaxial set (one sensitive to vertical motion and two sensitive to horizontal motion), with sensitivity to ground motion sharply peaked at .45 Hz. The fourth seismometer is sensitive to vertical motion, with peak sensitivity at 8 Hz. These instruments can detect vibrations of the lunar surface as small as  $\frac{1}{2}$  Å at maximum sensitivity.

Table 1.—*Locations and Installation Dates of the Stations of the Apollo Seismic Network*

Station	Date of Installation	Location	
		Latitude	Longitude
12	Nov. 19, 1969	3.04°S.	23.42°W.
14	Feb. 5, 1971	3.65°S.	17.48°W.
15	July 31, 1971	26.08°N.	3.66°E.
16	April 21, 1972	8.97°S.	15.51°E.

<sup>1</sup> Contribution No. 44 of the Marine Science Institute, Division of Solid Earth and Planetary Geophysics, University of Texas, Galveston, Texas.

Owing to the extreme quiet of the lunar surface, the instruments can be operated at peak magnification of approximately 20 million. This is two to three orders of magnitude higher than can normally be used on Earth. All but two of the 16 separate seismometers are presently operating. The short-period seismometer at station 12 has failed to operate since initial activation, and the long-period vertical component seismometer at station 14 became unstable after 1 yr of operation.

The following section summarizes the major findings from earlier work for the benefit of the reader unfamiliar with these results. A recent review of the results has been presented by Lammlein et al. (ref. 1).

## Brief Review of Previous Results

Prior to the first lunar landings, the seismic experiment team had anticipated that moonquakes, if extant, might originate along the large rill-like features that crisscross the lunar surface or along the fracture systems associated with the large maria basins. High-frequency signals that are possibly shallow moonquakes have, in fact, been recorded and are among the largest of the signals recorded to date. However, these high-frequency signals are extremely rare; 11 such events have been identified over a period of 3 yr. Much more numerous, but very small in magnitude (maximum Richter magnitudes of about 2), are moonquakes that occur at great depth. These are concentrated in a relatively thin zone at depths of between about 600 and 800 km. A third category of moonquakes has been recognized. These are small events that can be detected at each station at maximum ranges of a few tens of kilometers. The frequency of occurrence of these events is closely correlated with the lunar surface temperature cycle. These are almost certainly of thermal origin. Slumping of material along steep slopes or dislocations along fracture or bedding planes of material very near the surface caused by thermal stresses have been suggested as pos-

sible source mechanisms (ref. 2). These will not be discussed further here, except to remark that the mechanism leading to thermal moonquakes may represent an important erosional process on the lunar surface. The total annual energy release from moonquakes is estimated to be less than  $10^{15}$  ergs per year. This is about nine orders of magnitude lower than that of the Earth. If the sensitivities of the lunar seismographs were limited to the levels of their terrestrial counterparts, we would have recorded no moonquakes at all. Our conclusion would have been that the Moon is totally devoid of internal activity leading to quakes. Signals are recorded from several hundred meteoroid impacts per year at each station. By using the impacts from the third stages of the Saturn boosters as calibrations and a statistical method developed by James Dorman (described in ref. 3), the present meteoroid flux in the vicinity of the Moon has been estimated to be

$$\log N = -1.62 - 1.16 \log m$$

where  $N$  is the cumulative number of meteoroids of mass  $m$  (in grams) and greater which strike the Moon per year per square kilometer. This flux estimate is one to three orders of magnitude lower than those derived from earlier Earth-based measurements. However, it is in agreement with estimates derived from the distribution of crater sizes on the youngest lunar maria, assuming a plausible decrease in meteoroid flux between the time of maria formation and the present. Indeed, Wetherill (ref. 4) has pointed out that previous Earth-based flux estimates were too high by a factor of about 35 to be consistent with the crater size distributions observed on the maria. We estimate that a meteoroid of mass 7 to 10 kg can be detected by the Apollo Seismic Network from any point on the Moon. Thus, the Moon, when attached to a seismometer, has proven to be an unexpectedly good "sounding board" for the detection of meteoroid impacts. This results from a combination of two factors: the extremely high instrument sensitivities possible on the lunar surface and the unusually high efficiency of seismic wave propagation throughout most of the lu-

nar interior. The major weakness in the method thus far is the availability of only one calibration point (S-IVB impact energy). Obviously, a larger number of man-made impacts covering a wide range of impact energies would be highly desirable. Gault (personal communication) has pointed out that we may need to increase our flux estimate by a factor of 2 to correct for the probability of nonnormal angles of impact. It should also be noted that attempts to use near-range seismic sources (thumper, etc.) as calibrations for meteoroid impact signals recorded by the SPZ component lead to higher meteoroid flux estimates (ref. 2). The discrepancy between these two methods remains to be resolved.

Lunar seismograms differ markedly from typical Earth recordings. The most striking feature of lunar signals is their long duration. Examples are shown in figure 1. Impact-generated lunar signals have emergent beginnings, increase gradually to a maximum, and then slowly decay. Following the first one or two cycles of the P-wave, ground motion is very complex, with little or no correlation between any two components. The onset of the shear wave from near impacts (ranges less than 1000 km) cannot be identified with certainty. Coherent surface wave trains displaying dispersion have not been recognized in any recordings to date, although scattered surface waves undoubtedly contribute to the signals. The direction of propagation can rarely be determined from the particle motion at a single station. Thus, many analysis techniques found useful in terrestrial seismology cannot be applied to lunar signals. Signals from the deep moonquakes are generally less complex in the early part of the wave train than those from impacts. The largest amplitudes are clearly associated with the shear waves; however, the exact onset of the shear waves is difficult to identify. These unusual characteristics of lunar signals appear to be accounted for by assuming a high degree of heterogeneity, resulting in intensive scattering, and very low absorption of seismic wave energy in a thin surficial zone, referred to as

the scattering zone. Nakamura (ref. 5) has successfully described the envelope characteristics of lunar signals by using diffusion theory. His analysis shows that most of the scattering occurs in the outer few hundred meters of the Moon in which the  $Q$  of the medium must range between about 3000 and 5000. In fact, the extremely low absorption of seismic waves in this material is the dominant factor leading to the characteristics of lunar seismograms described above. Many

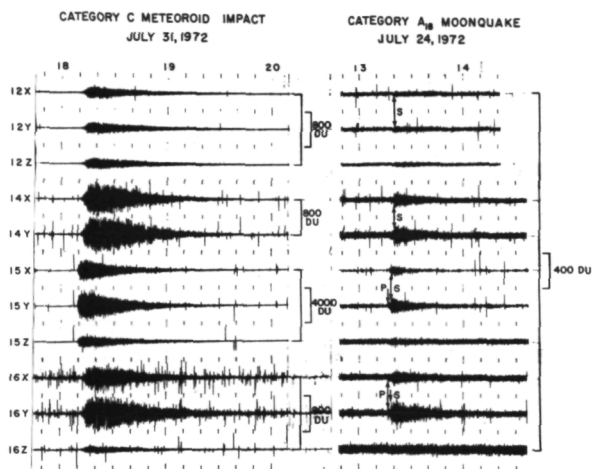


Figure 1.—Compressed time-scale records of long-period (LP) components for two natural seismic events recorded at four seismic stations. X and Y refer to the horizontal component seismometers; Z refers to the vertical component seismometers. Each successive trace deflection of an LP compressed time-scale record represents the sum of the absolute values of the differences between 40 successive data samples during consecutive, non-overlapping 6-s time intervals. Successive deflections are plotted on opposite sides of the zero baseline. The relative amplitudes of the signals are indicated by the brackets following each record. Tick marks are 10 min apart, and hours are labeled. The category  $A_{18}$  moonquake zone is located at the eastern border of Mare Serenitatis. For category A moonquakes, the direct shear wave S is prominent on seismograms from the horizontal seismometers. The direct compressional wave P is observed on seismograms of the largest category A moonquakes. The category C meteoroid impacted roughly 500 km north of station 15. The onsets of the direct compressional and shear waves can rarely be identified on LP seismograms of category C events.

terrestrial seismograms would possess the same characteristics as those of lunar seismograms if the absorption of seismic energy were reduced to lunar values. There is a growing body of laboratory data supporting our earlier contention that this marked contrast in absorption can be ascribed to the nearly complete absence of volatiles, principally water, in the outer shell of the Moon.

A seismic velocity model for the upper 150 km of the Moon has previously been defined (refs. 3 and 6) on the basis of observed traveltimes and amplitudes of body waves from nine impacts of S-IVB and LM space vehicles, combined with data from laboratory measurements on returned lunar samples. Seismic signals from these impacts were recorded at ranges from 9 km to 1750 km. Figure 2 shows a first-order model for the variation in the velocity of compressional waves, with depth consistent with the traveltimes of seismic waves from these manmade impacts and a meteoroid impact that occurred within the array. The most important feature of this model is the abrupt increase in velocity in the depth range between 50 and 55 km. By analogy with the Earth, we refer to the zone above this discontinuity as the crust and to the zone below as the mantle. Near the surface the velocity increases rapidly from a value of about 100 m/s measured in the regolith, reaching a value of between 6.3 and 7.0 km/s at the base of the crust. The rapid increase in velocity near the surface can be explained by the progressive compaction of materials so thoroughly fragmented that the velocity of propagation through them is determined primarily by its mechanical state rather than by its chemical composition. Velocities in the range from 6 to 7 km/s are appropriate for, but not restricted to, the rock types found to predominate in the lunar highlands (anorthositic gabbros and aluminous basalts). At the mantle boundary, the compressional wave velocity increases to about 8.1 km/s—a value appropriate for rocks of olivine-pyroxene composition. As shown by Kovach and Watkins (ref. 7), the velocity variation in the outer crust may be stepwise in some areas

where flows (ash or lava) have escaped complete obliteration, but the smooth variation shown in figure 2 appears to be a good approximation of the stepwise increase they infer for the region of the Apollo 17 landing site.

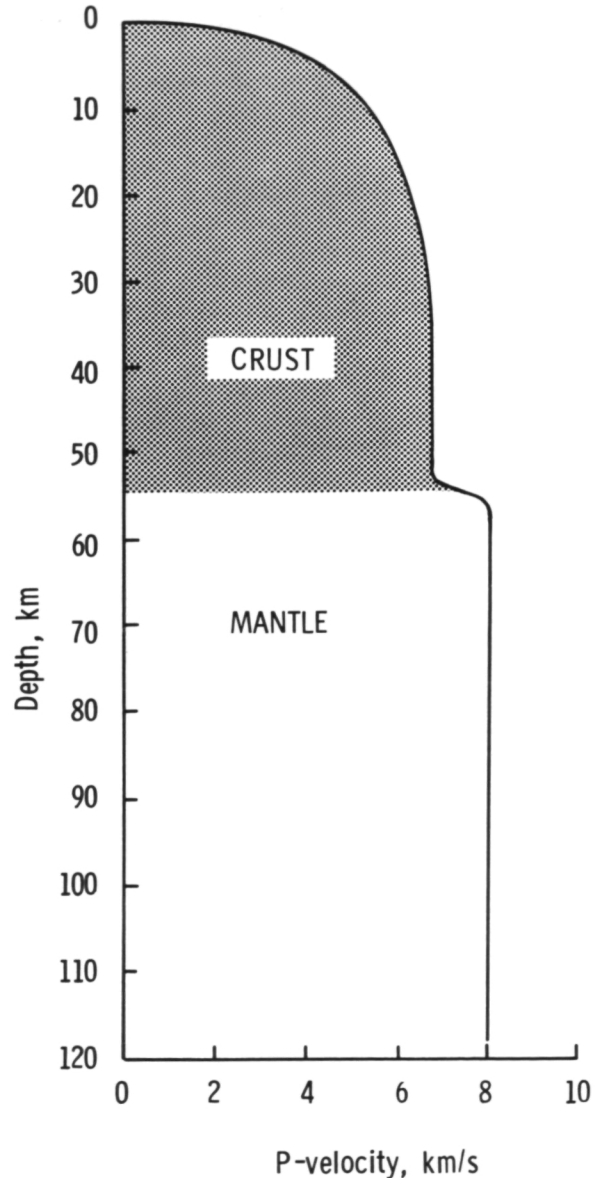


Figure 2.—Compressional wave velocity model based on seismic data from nine manmade impacts and one near meteoroid impact.

It was found soon after the installation of station 12 that moonquake signals could be grouped into sets, with members of each set having waveforms that match one another in detail. Moonquakes in each group occur at regular intervals, normally once per month, and at specific times during the lunar orbit. In some cases as many as three or four moonquakes of a given set will occur during a monthly cycle, but such multiple events occur over a relatively short interval of a few days or less. The repetitious character of these events strongly supports the hypothesis that they are moonquakes, each group of matching signals corresponding to an active zone or focus within the Moon at which the repeating moonquakes originate. Forty-one sets of signals, corresponding to 41 active foci, have been identified to date. Since the total number of moonquakes in the matching groups represent only about 10 percent of the several thousand moonquakes recorded to date, it is quite probable that many other active foci exist. However, the signals recorded from them are too small to permit detailed analysis of their waveforms.

Two tidal periodicities have been recognized in the moonquake activity patterns (variations in times-of-occurrence and amplitudes): 13.6 days and 206 days. The shorter period variation corresponds to the nodical or draconic month. The longer period is introduced by solar perturbation of the lunar orbit, which results in a cyclical variation of the Earth-Moon separation at times of perigee. A third periodicity, corresponding to the successive synchronizations of the anomalistic and nodical months and having a period of about 6 years, appears to be present. However, the sample length is not yet long enough to confirm this. It is evident that tides play a dominant role in the generation of moonquakes. However, with very few possible exceptions, the polarities of seismic signals from a given source are identical. This implies that the dislocation is progressive and not periodically reversed. Progressive dislocation suggests secular accumulations of strain periodically released by moonquakes. Weak convection within the

deep lunar interior or relaxation of tidal deformation as the Moon recedes from the Earth have been suggested as possible sources of secular accumulation of strain.

Using the velocity model described above, extrapolated to the depths of moonquakes, 27 of the active foci have been located. The epicentral locations are shown in figure 3. In nine cases the depth of focus was assumed in the calculation. The moonquake foci are concentrated in two narrow belts. Both belts are 100 to 300 km wide, about 2000 km long, and 600 to 800 km deep. (Earlier estimates placed the depth of the moonquake zone at between 800 and 1000 km.) Whether the apparent alignment into belts is real or a mirage that will disappear as more epicenters are located is not known. However, the distribution is certainly not random. The epicenters lie approximately along arcs of great circles that intersect at an angle of about 80 degrees. This pattern cannot be explained as a natural consequence of the distribution of seismic stations, nor do we know of any tidal stress component that would lead to such a pattern. In addition, no systematics in the relative times of occurrence of the moonquakes within a given belt have been discerned, except that peaks in the combined activity detected from all foci occur at average intervals of 13.6 days and are approximately in phase at all stations.

Only one moonquake epicenter has been located on the farside of the Moon. For signals from this source, it was noticed that shear waves were missing in the seismogram recorded at the most distant station for which the signal could be detected (station 14). Since shear waves from moonquakes are normally prominent at station 14, this observation remained a mystery until the phenomenon of missing, or greatly delayed, shear waves was observed in the records from a distant impact. Although other interpretations are possible, Nakamura et al. (ref. 8) found that these observations could be explained by assuming that partial melting begins in the present-day Moon at a depth of about 1000 km. (This boundary must be moved upward to a depth of about

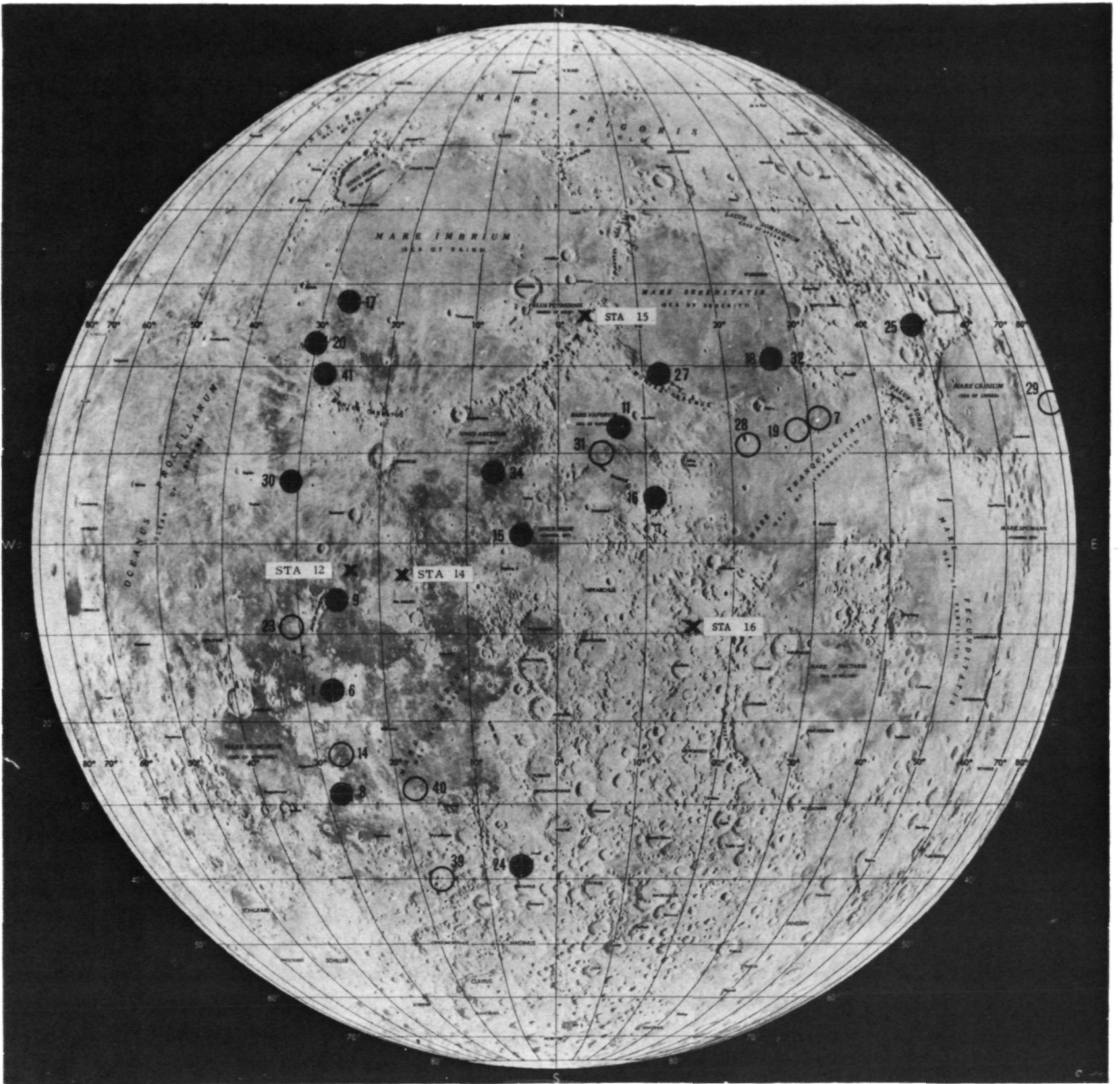


Figure 3.—Map of the nearside of the Moon locating the Apollo 12, 14, 15, and 16 seismic stations (table 1) and the category A moonquake epicenters. Solid circles indicate the foci for which the depth can be determined. Open circles correspond to cases in which data are not sufficient for determination of depth. In these cases a depth of 800 km was assumed to locate the epicenter. Note that epicenters 1 and 6 and 18 and 32 are so closely spaced that their separation cannot be distinguished at the scale plotted. One focus occurs on the farside of the Moon.

800 km according to the more recent results presented here.) Following the same line of reasoning, significant melting cannot be present in the crust and mantle at depth shallower than the moonquake zone, since high-frequency shear waves are prominent in the seismograms from all nearside moonquakes. Since little or no seismic activity has been detected above the moonquake zone and subsolidus temperatures are inferred, we refer to this dynamically inactive outer shell as the lithosphere and to the "weaker" central zone, in which partial melting is inferred, as the asthenosphere.

## Recent Results

### HIGH-FREQUENCY TELESEISMIC EVENTS

A set of seismic signals with unusual characteristics has recently been identified (ref. 9). They are distinguished from all other signals recorded at comparable ranges (greater than 1000 km) by their high-frequency content. Only 11 signals of this type, designated high-frequency teleseismic (HFT) signals, have been identified in the 3-year period for which data are available. Some of these are among the largest signals detected. Recordings for one of these events are shown in figure 4, along with representative signals from a moonquake and a meteoroid impact. The relatively high-frequency content of the HFT signal can be seen in this figure by comparing the amplitudes recorded by the long-period seismometers (LPX,Y,Z) with those recorded by the short-period seismometers (SPZ). The relatively large amplitude of the SPZ record for the HFT event indicates that most of the signal energy is at frequencies above 1 Hz; whereas frequencies below 1 Hz are dominant in signals for distant moonquakes and impacts. This comparison is made for a larger number of events in figure 5, where the ratio of the maximum signal amplitudes recorded by the SPZ and LPY (one of the long-period horizontal components) seismometers is plotted

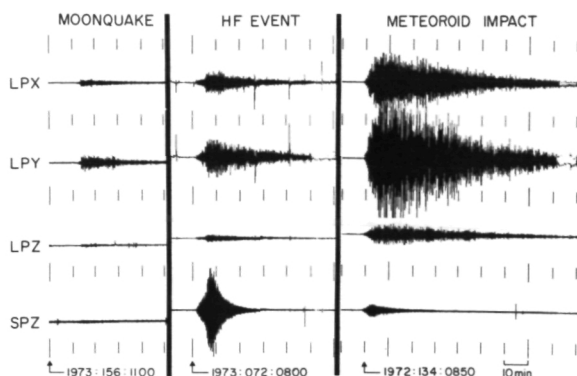


Figure 4.—Seismogram of a high-frequency teleseismic (HFT) event detected on March 13, 1973 (center), compared with those of a moonquake detected on June 5, 1973 (left: category  $A_1$ ), and a meteoroid impact detected on May 13, 1972 (right). All of these seismograms were recorded at the Apollo 16 station. LPX, LPY, and LPZ stand for three orthogonal components of a long-period instrument peaked at about 0.45 Hz. SPZ stands for a short-period vertical component peaked at 8 Hz. Note the relatively impulsive beginning of P- and S-wave arrivals of the HFT event, similar to those of the moonquake, and the large SPZ amplitude of the HFT event.

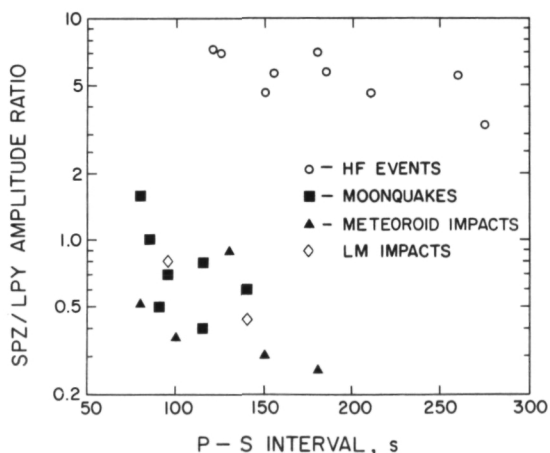


Figure 5.—SPZ/LPY amplitude ratio versus S-P time interval for the HFT events and selected other events recorded by the Apollo 14 station. A large amplitude ratio means a greater high-frequency content of a signal. Increasing S-P time corresponds to increasing distance from the station.

versus the time interval between the P-wave and S-wave arrivals for each signal. This time interval is a function of distance between the source and the seismic station—increasing time interval corresponding to increasing distance. The distinctive character of the HFT signals is evident in this plot.

The beginnings of the P-wave and S-wave trains are much more impulsive for HFT signals than those of typical meteoroid impact signals, suggesting that scattering near the source is much less for the HFT events than for normal surface sources. On the other hand, the predominance of shear waves in the signals from the most distant HFT events requires that the source be shallower than 300 km (ref. 9).

Several source mechanisms for these unusual signals are suggested: either they are generated by meteoroids that penetrate the scattering zone into more competent material below (200 to 300 meters), they are generated by impacts in areas where unusually competent and structurally homogeneous material lies close to the surface, or they are shallow moonquakes. The latter interpretation is favored. It is difficult to conceive of any process that would preserve isolated patches of the lunar surface relatively undisturbed by meteoroid impacts. If such regions do exist, gradational cases would be expected, resulting in a broad spectrum of signal characteristics instead of the sharp division between signal classes observed. On the other hand, the existence of some shallow moonquake activity in a cooling planet would be expected.

## STRUCTURE AND STATE OF THE DEEP LUNAR INTERIOR

Information on the structure and state of the deep lunar interior is derived principally by analysis of seismic signals from distant impacts and moonquakes. As noted above, meteoroid impact signals are so emergent that it is rarely possible to pick the onset of the P-wave with certainty, and the onset of shear waves can be separated out from the

compressional wave train only in the signals from distant impacts. Signals from four of the largest impacts and two of the HFT events have been selected as suitable for the present analysis. The traveltime curves for these events, as given by Nakamura et al. (ref. 10), are shown in figure 6. These data can be inverted by the Wiechert-Herglotz method to give seismic velocities as a function of depth, assuming that velocity gradients are not so large as to invalidate the method. However, several points can be made by inspection of these curves without further analysis. First, we note that the curve for shear (S) waves departs markedly from the curve for compressional (P) waves at a range of about  $85^\circ$  (2600 km), corresponding to maximum depths for the S-wave ray path of about 300 to 400 km. The velocity of shear waves must begin to decrease sharply (i.e., Poisson's ratio begins to increase) in this depth range. Secondly, the P-wave traveltime for the most distant point is delayed by about 120 s from the value expected by smooth extrapolation of the curve. This indicates that the velocity of P-

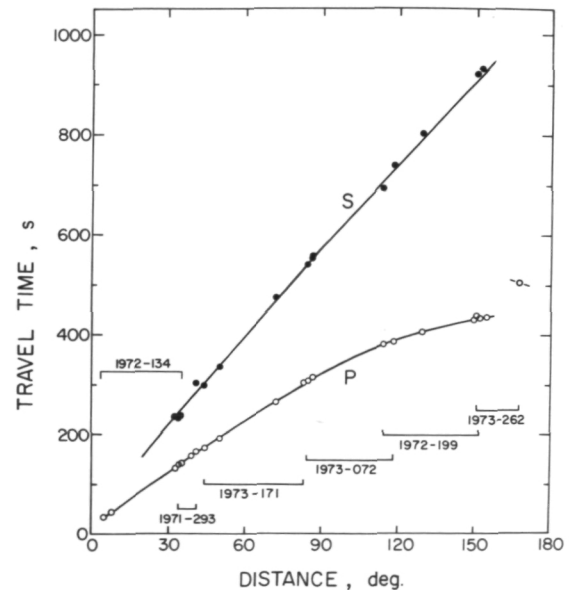


Figure 6.—Travel-time data for compressional (P) and shear (S) waves recorded from four distant impacts and two HFT events.

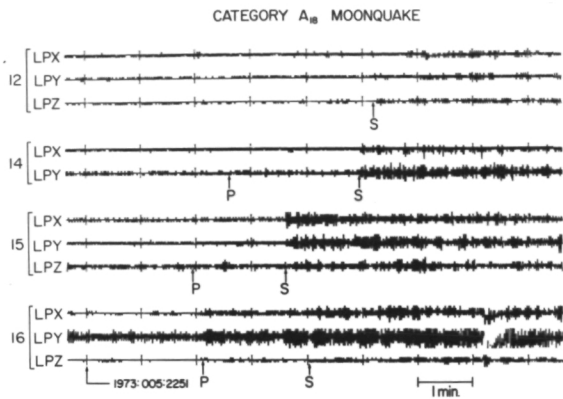


Figure 7.—Four-station expanded time scale play-outs of a category  $A_{18}$  moonquake detected at 22:53 hours on January 5, 1973. X and Y refer to LP horizontal component seismometers; Z to the LP vertical component seismometers. Tick marks are 1 min apart. These signals are typical of moonquakes recorded at each of the stations. The direct shear wave (S) is prominent on the horizontal component seismograms at all of the stations. The direct compressional wave (P) is also observed at stations 14, 15, and 16.

waves decreases abruptly at depths of between 1380 and 1570 km.

Below the zone of abrupt shear-wave decrease, the Wiechert-Herglotz method cannot be applied for shear waves with confidence, and signals from moonquakes that originate beneath this zone must be used. Signals from one of the moonquakes used in this analysis are shown in figure 7. Combining the traveltime data from deep moonquakes with the data of figure 6, the model shown schematically in figure 8 has been derived. For purposes of discussion, it is convenient to divide the lunar interior into five major zones:

### Zone 1—The Crust

Zone 1 represents a layer approximately 55 km thick in the region of stations 12 and 14. If the crust is a global feature, as suggested by several lines of evidence (ref. 1), it is probably quite variable in thickness, with thickness of the backside crust substantially greater than that of the nearside (ref. 11).

The crustal velocities are appropriate for the plagioclase-rich materials inferred from sample analysis, possibly grading from anorthositic material at the top to more gabbroic material at depth.

### Zone 2—The Upper Mantle

Zone 2 is approximately 250 km thick, with a compressional wave velocity of about 8.1 km/s at the top, decreasing to about 7.8 km/s at the bottom. Possible compositions of this zone can be inferred from the velocities and densities corresponding to the model of figure 8. Based upon geochemical considerations (ref. 12), olivine and pyroxene are the most probable constituents of the rocks of the upper mantle. Curves of velocity versus density for these minerals are given in figure 9, along with the values derived from our preliminary model, assuming a uniform composition for the upper mantle (i.e., the velocity decrease with depth in the upper mantle is due to increasing temperature with depth). The experimental values

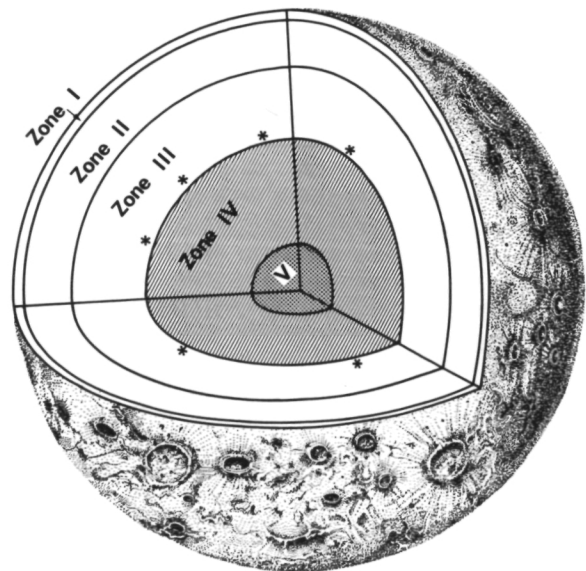


Figure 8.—Pictorial representation (drawn approximately to scale) of the internal structure of the Moon as described in the text. X marks indicate the zone of deep moonquakes.

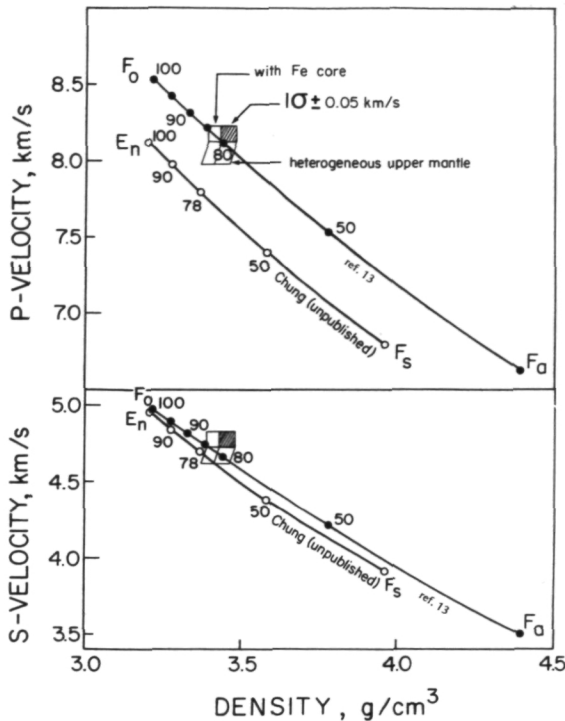


Figure 9.—Density versus velocity (corrected to standard temperature and pressure) calculated from the seismic data of figure 6 for the upper mantle (zone 2) of the Moon. Compressional and shear-wave data for the olivine ( $F_o$ — $F_a$ ) series (ref. 13) and the orthopyroxene ( $E_n$ — $F_s$ ) series (Chung, personal communication, 1974) are shown for comparison. The calculations permit variations in the various lattice dynamical parameters over ranges approximate for rocks of mafic composition. Calculations have been made for two cases. (1) The crosshatched block corresponds to the assumption that the composition of the upper mantle is uniform throughout, i.e., that the effects of temperature and pressure balance to give the experimentally determined velocity-depth functions. This requires a velocity gradient of 4 to 5° C/km in the upper mantle, (2) The open block below shows the change introduced by decreasing the temperature gradient to between 2 and 3° C/km. For this case, the intrinsic velocity and density must decrease slightly with depth. From this comparison, a composition close to the magnesian end of the olivine series (80 percent forsterite) is suggested for the upper mantle. For both cases described above, the effect of including an iron core (zone 5) of density 7.5 g/cc and a maximum radius of 360 km is also shown.

for the upper mantle thus derived are in good agreement with the olivine data (80 to 85 percent forsterite). The calculated points are shifted slightly to the left if an iron-sulphide core (zone 5) is assumed. The assumption of constant composition requires a temperature gradient of 4 to 5° C/km for the upper mantle. Alternatively, the traveltime data can be satisfied by assuming a variation from magnesian olivine at the top to more pyroxenitic material below and reduction of the temperature gradient to between 2 and 3° C/km. Walker et al. (ref. 14) have pointed out that a mafic cumulate of thickness corresponding to that inferred here for the upper mantle (about 250 km) might be expected if a plagioclase-rich crust 50 to 60 km thick is present.

### Zone 3—The Middle Mantle

This zone, extending from about 300 to 800 km, is characterized chiefly by the reduced velocity of shear waves (3.6 to 4.0 km/s) within it. It is likely that the compressional wave velocity is also decreased slightly in this layer, but this cannot be resolved with the available data. Thus, the material of zone 3 must have a high Poisson's ratio (0.34 to 0.35) compared to that of the material above in which the Poisson's ratio is approximately 0.25. One possible interpretation is that this zone represents primitive lunar material below the zone of initial melting that produced zones 1 and 2. Mare basalts may have been produced by partial melting within zone 3, 3.2 to 3.8 b.y. ago in accordance with the proposals of Duba and Ringwood (ref. 12) and others. Moonquakes are concentrated within a relatively thin zone at the base of zone 3, in a depth range of from 600 to 800 km. Because high-frequency shear waves are recorded from all of these sources (except the farside focus), we can say immediately that widespread melting in zones 1, 2, and 3 is not possible, i.e., temperatures in these zones must be subsolidus. In addition, there is little or no scattering of seismic waves in zone 3. Thus, if

this represents an accumulation of primitive materials, either individual blocks are small compared to a wavelength (less than about 1 km in dimension), the elastic properties of the individual blocks do not vary appreciably, or any inhomogeneities have been removed by subsequent melting.

There is some evidence that the transition from zones 2 to 3 may be relatively sharp. A prominent phase, designated R in figure 10, has been identified in the wavetrains of the largest moonquake signals. The relative arrival times for this phase can be explained by assuming that the phase is generated by conversion from S to P at an interface located at a depth of about 300 km, the approximate depth for the boundary between zones 2 and 3 derived from shear-wave travel-time data. Similar mode conversions have been tentatively identified in records from deep earthquakes (ref. 16).

#### Zone 4—The Lower Mantle

This zone is characterized chiefly by the absence of identifiable shear waves for events in the distance range for which shear waves would enter this zone. This can be ascribed to (1) a sharp decrease in shear-wave velocity at the top of the zone, leading to a shadow zone for shear waves, or (2) high attenuation of shear waves within this zone.

The latter interpretation is favored for the following reasons. First, we must explain the concentration of moonquake activity, closely correlated with lunar tides, immediately above this zone. Calculation of tidal energy density as a function of depth shows that a sharp maximum is introduced in the depth range of moonquakes if a zone of much "weaker" material (zone 4) is introduced below (ref. 16). Second, the velocity of P-waves cannot decrease more than 0.2 to 0.3 km/s within this zone. A greater decrease in compressional wave velocity would be expected to accompany the sharp decrease in the shear-wave velocity required to produce an optical shadow zone. To explain these observations, Nakamura et al. (ref. 8) have argued that partial melting is probable in the lunar mantle. If so, a temperature of approximately 1500°C is inferred for the top of zone 4, assuming a mafic composition.

#### Zone 5—The "Core"

This zone is characterized by a sharp decrease in the velocity of P-waves beginning at a depth of from 1380 to 1570 km. The inferred P-wave velocity for this zone is about 5 km/s, suggesting that the material of this zone is completely molten. Unless the material of zone 5 is more dense than that of zone 4, convective instability between zones

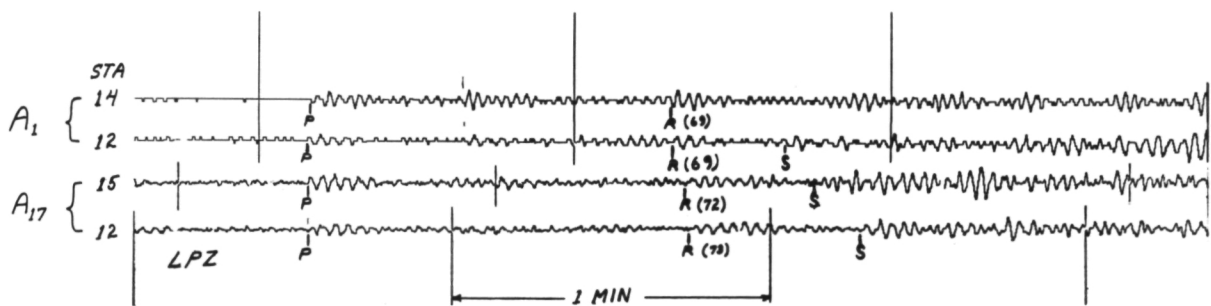


Figure 10.—Seismograms from the long-period vertical component for two moonquakes, showing a phase (R) that may correspond to conversion from shear wave (S) energy to compressional wave (P) energy at an interface at a depth of about 300 km (the boundary between zones 2 and 3).

4 and 5 would result. It is suggested that zone 5 represents a molten core of iron sulphide in accordance with the models earlier suggested on geochemical grounds by Brett (ref. 17) and Duba and Ringwood (ref. 12). If the composition of the core is iron sulphide, it represents less than 1 percent of the total mass of the Moon and falls easily within moment-of-inertia constraints. However, this interpretation must be regarded as quite tentative pending the acquisition of more seismic data pertinent to the properties of this zone.

## Conclusions

An iron sulphide core of radius 200 to 300 km, as suggested by present seismic data, may have been the source of an early dipole field that magnetized lunar surface rocks.

If accretional energy were responsible for melting the outer shell of the Moon to a depth of about 300 to 350 km to produce the crust and upper mantle, very short accretion times are required—probably less than 10 000 years (ref. 12).

The low level of lunar seismicity and its concentration at great depth compared to the Earth now appear to be explained by the differences in thickness of the lithospheric shells and internal thermal energy of these two planets. The lunar lithosphere is simply too thick (about 800 km) to be disrupted by the relatively weak convective motion that might be induced by temperature gradients below. In the absence of this source of seismic activity, i.e., collisions between lithospheric plates, dislocations induced by tidal deformation of the Moon, are the dominant mechanisms for generation of quakes. Assuming that the Moon is cooling (contracting) slightly at present, as suggested by the thermal models of Toksöz and Solomon (ref. 18), the accumulation of compressional stress in the lithosphere would be expected to result in moonquakes at shallow depth. The few, relatively energetic events of unusually high-frequency (HFT) signals that have been detected may be explained in this way.

## Acknowledgment

This research was supported by the National Aeronautics and Space Administration under contract NAS 9-13143.

## References

1. LAMMLEIN, D., G. LATHAM, J. DORMAN, Y. NAKAMURA, AND M. EWING, Lunar Seismicity, Structure, and Tectonics. *Rev. Geophys. and Space Phys.*, Vol. 12, 1974, pp. 1-21.
2. DUENNEBIER, F., AND G. SUTTON, Thermal Moonquakes. *J. Geophys. Res.*, Vol. 79, in press, 1974.
3. LATHAM, G., M. EWING, J. DORMAN, Y. NAKAMURA, F. PRESS, T. TOKSÖZ, G. SUTTON, F. DUENNEBIER, AND D. LAMMLEIN, Lunar Structure and Dynamics—Results from the Apollo Passive Seismic Experiment. *The Moon*, Vol. 7, 1973, pp. 396-421.
4. WETHERILL, G., Of Time and the Moon. *Science*, Vol. 173, 1971, pp. 383-392.
5. LATHAM, G., M. EWING, F. PRESS, G. SUTTON, J. DORMAN, Y. NAKAMURA, N. TOKSÖZ, R. WIGGINS, J. DERR, AND F. DUENNEBIER, Apollo 11 Passive Seismic Experiment. *Geochimica et Cosmochimica Acta*, Supplement 1, Vol. 34, 1970, pp. 2309-2320.
6. TOKSÖZ, N., F. PRESS, A. DAINITY, K. ANDERSON, G. LATHAM, M. EWING, J. DORMAN, D. LAMMLEIN, G. SUTTON, F. DUENNEBIER, AND Y. NAKAMURA, Velocity Structure and Properties of the Lunar Crust. *The Moon*, Vol. 4, 1972, pp. 490-504.
7. KOVACH, R., AND J. WATKINS, Apollo 17 Seismic Profiling: Probing the Lunar Crust. *Science*, Vol. 180, 1973, pp. 1063-1064.
8. NAKAMURA, Y., D. LAMMLEIN, G. LATHAM, M. EWING, J. DORMAN, F. PRESS, AND N. TOKSÖZ, New Seismic Data on the State of the Deep Lunar Interior. *Science*, Vol. 181, 1973, pp. 49-51.
9. NAKAMURA, Y., J. DORMAN, F. DUENNEBIER, M. EWING, D. LAMMLEIN, AND G. LATHAM, High-Frequency Lunar Seismic Events. *Proc. Fifth Lunar Science Conference*, in press, 1974.
10. NAKAMURA, Y., G. LATHAM, J. DORMAN, F. DUENNEBIER, M. EWING, AND D. LAMMLEIN, Seismic Evidence on the Structure of the Deep Lunar Interior—A Progress Report. *Geophys. Res. Letters*, in press, 1974.
11. KAULA, W., G. SCHUBERT, R. LINGENFELTER, W. SJOGREN, AND W. WOLLENHAUPT, Lunar Topography from Apollo 15 and 16 Laser Altimetry. *Geochimica et Cosmochimica Acta*, Supplement 4, Vol. 3, 1973, pp. 2811-2819.

12. DUBA, A., and A. RINGWOOD, Electrical Conductivity, Internal Temperatures, and Thermal Evolution of the Moon. *The Moon*, Vol. 7, 1973, pp. 356-376.
13. CHUNG, D., Elasticity and Equations of State of Olivines in the  $Mg_2SiO_4$ - $Fe_2SiO_4$  System. *Geophys. J. R. Astron. Soc.*, Vol. 25, 1971, pp. 511-538.
14. WALKER, D., T. GROVE, J. LONGHEI, E. STOLPER, AND J. HAYS, Origin of Lunar Feldspathic Rocks. *Earth Planet. Sci. Letters*, Vol. 20, 1973, pp. 325-336.
15. JORDAN, T., Crust and Upper Mantle Structure From SP Phases. *Trans. Am. Geophys. Union*, Vol. 55, 1974, p. 359.
16. LAMMLEIN, D., AND G. LATHAM, Moonquakes and Tides. *Geological Soc. Am. Abs.*, Vol. 6, No. 3, 1974, p. 299.
17. BRETT, R., Sulphur and the Ancient Lunar Magnetic Field, *Trans. Am. Geophys. Union*, Vol. 53, 1972, p. 723.
18. TOKSÖZ, N., AND S. SOLOMON, Thermal History and Evolution of the Moon. *The Moon*, Vol. 7, 1973, pp. 251-278.